Available online at www.sciencedirect.com
SCIENCE DIRECT®
Bioelectrochemistry 62 (2004) 107–113
Bioelectrochemistry
www.elsevier.com/locate/bioelechem

The cooperative role of membrane skeleton and bilayer in the mechanical behaviour of red blood cells

Saša Svetina[a,b,*], Drago Kuzman[a], Richard E. Waugh[c], Primož Ziherl[b,d], Boštjan Žekš[a,b]

[a] Institute of Biophysics, Faculty of Medicine, University of Ljubljana, Lipičeva 2, SI-1000 Ljubljana, Slovenia
[b] Jožef Stefan Institute, Jamova 39, SI-1000 Ljubljana, Slovenia
[c] Department of Pharmacology and Physiology, School of Medicine and Dentistry, University of Rochester, 601 Elmwood Ave., Box 711, Rochester, NY 14642-0001, USA
[d] Department of Physics, University of Ljubljana, Jadranska 19, SI-1000 Ljubljana, Slovenia

Received 30 May 2003; received in revised form 19 August 2003; accepted 19 August 2003

Abstract

Red blood cell (RBC) shape, behaviour and deformability can be consistently accounted for by a model for the elastic properties of the RBC membrane that includes the elasticity of the membrane skeleton in dilation and shear, and the local and nonlocal resistance of the bilayer to bending. The role of the corresponding energy terms in different RBC shape and deformation situations is analyzed. RBC shape transformations are compared to the shape transformations of phospholipid vesicles that are driven by the difference between the equilibrium areas of the bilayer leaflets (ΔA_0). It is deduced that the skeleton energy contributions play a crucial role in the formation of an echinocyte. The effect of a transformation of the natural biconcave RBC shape into an echinocyte on its resistance to entry into capillary-sized cylindrical tubes is analyzed. It is shown that, during the aspiration of an echinocyte into a pipette, there are two competing skeleton deformation effects, which arise due to skeleton density changes, one due to spicule formation and the other due to deformation induced by micropipette aspiration. Furthermore, the shift of the observed dependence of the projection length on the aspiration pressure of more crenated cells towards higher aspiration pressures can be accounted for by an increase of the equilibrium area difference ΔA_0 and consequent modification of the nonlocal contribution to the cell elastic energy.

Keywords: Red blood cells; Deformability; Shapes; Membrane elastic properties; Echinocyte; Micropipette aspiration

1. Introduction

The elastic properties of the red blood cell (RBC) membrane influence both RBC shape formation as well as the response of this cell to different external stresses, i.e., its deformability. The RBC membrane consists of the phospholipid bilayer containing integral membrane proteins and the underlying membrane skeleton. The subject of this work is to demonstrate that these two parts of the RBC membrane affect its elastic behaviour in a cooperative manner.

A considerable insight has been already gained into the structure of RBC membrane constituents, such as spectrin [1] and the RBC membrane organization and microelasticity [2]. The latter results are particularly important for the interpretation of differences between the mechanical behaviour of different RBC membrane mutants and transgenically engineered mice that lack specific RBC membrane proteins. They can also be used for further elaboration of the theoretical links between structural details of the membrane constituents and macroscopic membrane properties such as the elastic moduli [3,4]. Recently, the elastic behaviour of the RBC membrane was studied also at a purely macroscopic level, with the aim to employ well-established mathematical descriptions of RBC membrane elasticity in the interpretation of RBC shapes and deformability. In this work, we shall survey some of these studies, in particular the continuum mechanics description of the echinocyte shapes [5], the membrane mechanics basis of the bilayer couple hypothesis [6] and echinocyte deformability [7].

The primary interest of cited papers [5–7] was in revealing which independent elastic deformational modes have to

* Corresponding author. Institute of Biophysics, Faculty of Medicine, University of Ljubljana, Lipičeva 2, SI-1000 Ljubljana, Slovenia. Tel.: +386-1-543-7600; fax: +386-1-431-5127.
E-mail address: sasa.svetina@biofiz.mf.uni-lj.si (S. Svetina).

1567-5394/$ - see front matter © 2003 Elsevier B.V. All rights reserved.
doi:10.1016/j.bioelechem.2003.08.002

be included minimally for a description of the shape and deformability behaviour of RBC of a given composition, which would wholly describe the response of the system to different physical and chemical perturbations. Physical perturbations relate to different external forces that act on RBC, e.g., aspiration pressure in the pipette experiment or forces due to the velocity gradient in a rheometer. Chemical perturbations include the effects on the equilibrium areas of different layers that compose the RBC membrane. The equilibrium leaflet areas play a role in determining membrane deformation in response to applied forces and are included in mathematical descriptions of the membrane response to applied forces. These areas are of interest in connection with the bilayer couple interpretation [8] of the stomatocyte–discocyte–echinocyte sequence of RBC shapes (Fig. 1A). Thus, the bilayer couple model explains these isovolumic RBC shape transformations by the asymmetric changes of the areas of the layers of the bilayer part of the red blood cell membrane. Within the realm of the bilayer couple model, the shape transformations of the RBC can be compared with the shape behaviour of phospholipid vesicles. The RBC shape transformation from the discocyte shape into the stomatocyte shape seems to be identical to the corresponding vesicle shape transformation, as shown in Fig. 1A and B. These shape transformations can be interpreted in terms of a decrease of the difference between the areas of the outer and the inner membrane layers [11,12]. On the other hand, it can also be seen in Fig. 1A and B that, at area differences which are larger than the discocyte area difference, RBCs transform into echinocytes and, in this

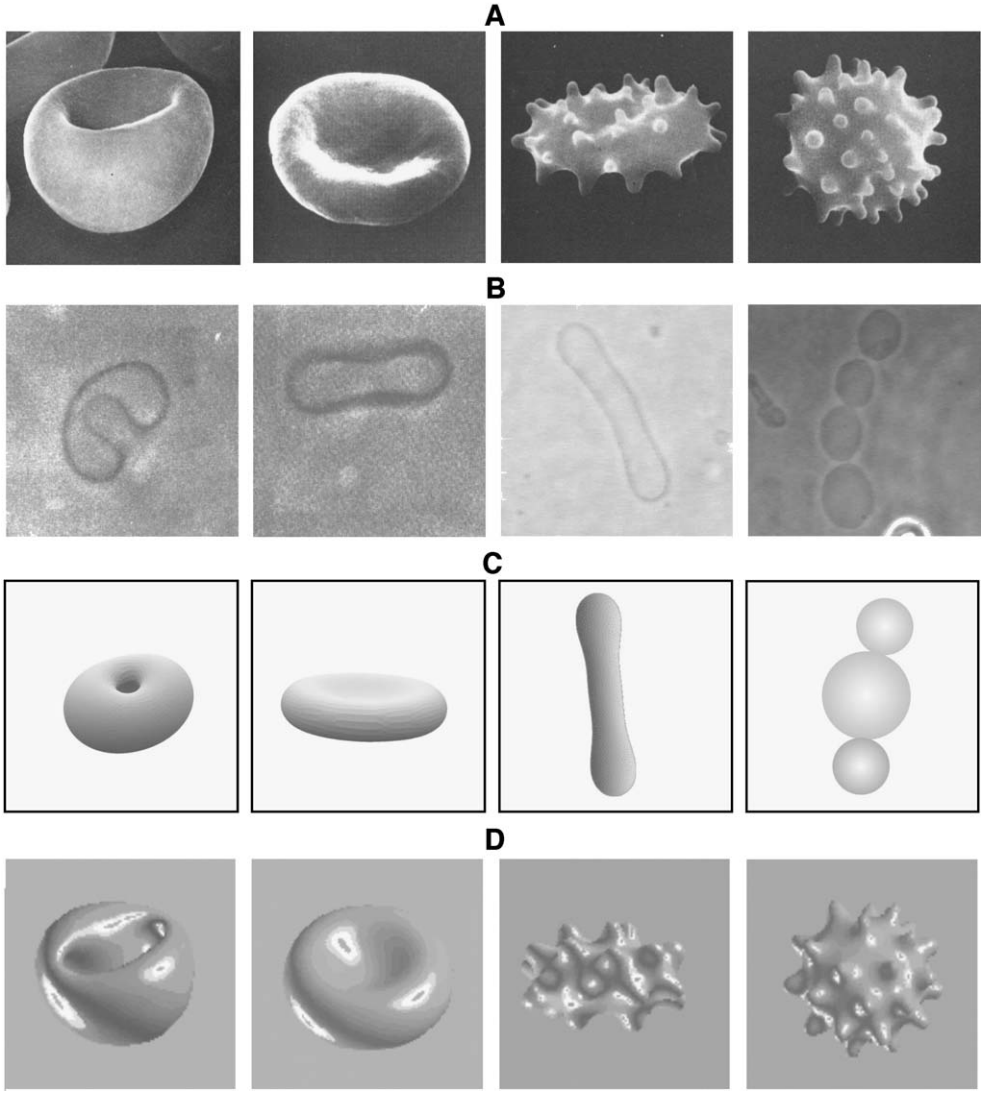

Fig. 1. Shapes of red blood cells and phospholipid vesicles. (A) RBCs observed at different conditions that determine the difference between the equilibrium areas of the outer and the inner leaflet of the bilayer part of the RBC membrane (from left to right): stomatocyte, discocyte, echinocyte I, echinocyte III (taken from Bessis [9]). (B) Examples of phospholipid vesicle shapes obtained experimentally by Käs and Sackmann [10] (the first two shapes) and in our laboratory (the second two shapes, Janja Majhenc, unpublished). (C) Phospholipid vesicle shapes obtained theoretically by minimization of Eq. (1) for different values of the equilibrium area difference ΔA_0. (D) RBC shapes predicted theoretically [6] for different values of ΔA_0.

region, they do not follow the shape course of phospholipid vesicles characterized by their tendency to form shapes composed of connected spherical parts.

As already stated, in order to obtain a consistent interpretation of RBC shape and deformability behaviour, it is necessary to include the elasticity contributions both from the membrane bilayer and the membrane skeleton. These were shown to be [5–7], at constant membrane surface area, the area expansivity and shear of the membrane skeleton, and local and nonlocal bending of the bilayer. The emphasis in this work will be in elucidating the reasons for including all these described deformational modes. We shall discuss separately first the aspects of the membrane bilayer and then the aspects of the membrane skeleton. The description of the echinocyte shape and deformability will be given next and, in the discussion section, we shall also present some general implications about the functional role of the RBC membrane skeleton.

2. The elasticity of the bilayer and shapes of phospholipid vesicles

The bilayer part of the RBC membrane and phospholipid membranes share the structural feature that they are both composed of two leaflets that are in contact but can relax lateral stresses independently. Their elastic properties must be therefore describable in terms of the same deformational modes. The comparison of the shape behaviour of phospholipid vesicles and RBCs can thus be indicative of the role of the membrane skeleton in the RBC shape formation. Here, we shall review briefly the basics of the bilayer elasticity and of the phospholipid vesicle shape behaviour.

The mechanical response of phospholipid vesicles is determined by the bilayer area expansivity, and the local and nonlocal bending [13–16]. The energy required to expand or compress the bilayer area is several orders of magnitude larger than the bilayer bending energy and therefore surface area (A_0) can be considered to be constant during vesicle shape transformations. The sum of the local (W_b) and nonlocal (W_r) bending energies is

$$W_b + W_r = \frac{k_c}{2}\int (c_1 + c_2 - c_0)^2 dA + \frac{k_r}{2h^2 A_0}(\Delta A - \Delta A_0)^2, \quad (1)$$

where in the local bending energy term k_c is the local bending modulus, c_1 and c_2 are the principal curvatures and c_0 is the spontaneous curvature. In the nonlocal bending energy term, k_r is the nonlocal bending modulus, h is the distance between the neutral surfaces of the two leaflets, ΔA is the difference between the neutral surface areas of the outer and the inner bilayer leaflets, which is equal to $\Delta A = h\int(c_1 + c_2)dA$ being thus defined by the vesicle shape, and ΔA_0 is the corresponding difference between the equilibrium (relaxed) areas of these leaflets, being thus determined by the leaflet compositions. Nonlocal bending energy has to be included because in general ΔA is not equal to ΔA_0.

In Fig. 1C are shown some characteristic shapes, which can be predicted [11,12] on the basis of the minimisation of Eq. (1) for different values of ΔA_0, and at constant membrane area and vesicle volume. They were calculated numerically using surface evolver [17]. The comparison of experimental (Fig. 1B) and theoretical (Fig. 1C) phospholipid vesicle shapes shows a satisfying agreement.

3. The elastic properties of the skeleton and its axisymmetric deformation

Different shape behaviour of phospholipid vesicles and RBCs at values of the parameter ΔA_0 that are higher than the discocyte value can be understood by the influence of the membrane skeleton [18]. The role of the membrane skeleton was originally implicated from studies of RBC deformability. Early studies of micropipette aspiration of the RBC have already indicated the crucial role that membrane shear deformation plays in RBC deformability [19]. These analyses were performed under the assumption that the skeleton is incompressible. More recently, Discher et al. [20], using fluorescence to image the deformation of the skeleton, demonstrated that the skeletal density of the pipette-aspirated membrane is nonuniform. Based on this evidence, Mohandas and Evans [3] and Boey et al. [4] developed elastic constitutive models of the membrane that account for the skeleton area expansivity.

The membrane skeleton is considered to be two-dimensional and to be free to move only in lateral directions. It is assumed that it does not contribute to the nonlocal bending of the membrane because the area expansivity modulus of the skeleton is four orders smaller than that of the bilayer [20]. The expression for the elastic energy of the skeleton is not trivial because the elastic response is nonlinear at large deformations [20–22]. The corresponding energies differ at large deformations, while at small extensional ratios they are all proportional to the sum of invariant terms $(\lambda_1 - \lambda_2)^2/2$ and $(\lambda_1 + \lambda_2 - 2)^2/2$, where the first term describes shear deformation (W_μ) and the second area expansivity (W_K):

$$W_\mu + W_K = \frac{\mu}{2}\int (\lambda_1 - \lambda_2)^2 dA_0 + \frac{K}{2}\int (\lambda_1 + \lambda_2 - 2)^2 dA_0, \quad (2)$$

with μ the shear modulus and K the area expansivity modulus. Deformations are given in terms of the extension ratios λ_1 and λ_2 that describe extensions of a relaxed skeleton patch in the two perpendicular principal directions.

The effects of the skeleton deformation will be illustrated here by considering a simple system in which a flat

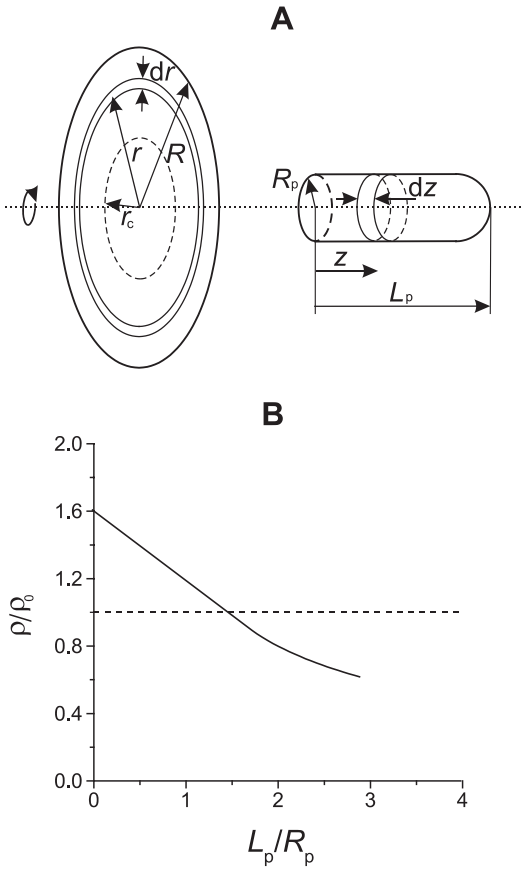

Fig. 2. Determination of the axisymmetric deformation of the RBC membrane skeleton. (A) Skeleton is deformed from a flat circular patch with the radius R to the tube with the radius R_p and the semispherical cap of the same radius. The circle with the radius r_c separates the outer part of the patch that is deformed into the tube from the central part that is deformed into the spherical cap. The meanings of other symbols are given in the text. A material point is mapped from its location in the undeformed membrane (left) at radius r to its location in the deformed membrane (right) at the coordinate z. The axis of symmetry is shown with dotted lines. (B) The dependence of the skeleton area density (ρ) relative to its density in the relaxed state (ρ_0) on the distance from the tube entrance. Above the dotted line, the skeleton is condensed; below the dotted line, it is expanded.

circular patch of the relaxed skeleton is displaced into the tube and in this way deforms into a cylinder with a spherical cap (Fig. 2A). The axis of symmetry is preserved in this deformation. Also preserved are the relative positions of the skeleton elements. It is therefore possible [7] to map the positions into which each point of the relaxed skeleton is displaced or vice versa. When considering as an example the deformation of the outer section of the circular patch into the cylinder (Fig. 2A), the area element $2\pi r\mathrm{d}r$ is displaced into the area element $2\pi R_p\mathrm{d}z$, and the skeleton is deformed such that the extensional ratios are:

$$\lambda_1 = \frac{R_p}{r} \text{ and } \lambda_2 = \frac{\mathrm{d}z}{\mathrm{d}r}. \tag{3}$$

It is assumed that the skeleton elastic energy in its relaxed state is zero. The total skeleton deformational energy (Eq. (2)) can then be expressed as

$$W = \pi \int_0^{L-R_p} \left[\mu \left(\frac{R_p}{r} - \frac{1}{r'} \right)^2 + K \left(\frac{R_p}{r} + \frac{1}{r'} - 2 \right)^2 \right] r r' \, \mathrm{d}z \tag{4}$$

where $r' = \mathrm{d}r/\mathrm{d}z$.

The skeleton deforms in a way that its elastic energy (Eq. (4)) increases minimally. The corresponding deformation can be obtained using a variational approach to minimise the energy (Eq. (4)) and thus find the mapping function $r(z)$ for which the skeleton energy is smallest. Such a mapping function can be conveniently obtained by solving the corresponding Euler–Lagrange equation [7].

In order to map the whole circular patch in Fig. 2A, its central part is mapped in an analogous way into the spherical cap. Because the area of the lipid part of the membrane remains constant, the total area of the deformed skeleton is the same as in the relaxed state. However, the relative proportion of the resting skeleton that is either displaced into the spherical cap or into the cylinder does not necessarily correspond to the relative proportions of the areas.

It is assumed that relaxed skeleton density is uniform with the density ρ0. Then, it cannot be uniform in the deformed state. The relative skeleton density at a point on the deformed cell is defined as:

$$\frac{\rho}{\rho_0} = \frac{1}{\lambda_1 \cdot \lambda_2}. \tag{5}$$

The resultant dependence of the skeleton density on the position on the cylinder is shown in Fig. 2B. The behaviour is consistent with the measurements of Discher et al. [20], who showed that the deformation of the membrane during pipette aspiration causes lateral redistribution of the membrane skeleton such that, in regions where the shear deformation is large, the density is larger than the relaxed density, and where shear deformation is small, the density is also small. This effect can be interpreted on the basis of energy minimisation in response to axisymmetric deformation. As the membrane is pulled into the pipette, each section of the membrane must decrease its circumference to $2\pi R_p$. If the area of the section remained constant, the skeleton would have to extend appreciably in the direction of the pipette axis. However, it is energetically more favourable for the system to decrease the energy of shear deformation by increasing its local density, thus trading an increase in dilational energy for a larger decrease in shear energy. Because the RBC skeleton is attached to the lipid bilayer, there is a constraint on the total skeleton surface area, requiring that when there is condensation of the skeleton in regions where shear deformation is high, dilation must occur

in regions where shear deformation is low. The effect is more pronounced when larger changes of the radial distances occur in the shape transformation. Such are the shape transformations both in RBC pipette aspiration and in the echinocyte spicule formation. The situation is different in the RBC discocyte–stomatocyte shape transformation where deformations of the skeleton are not large because the radial distances of different displaced skeletons in stomatocytes do not differ appreciably from the corresponding radial distances in the discocytes.

4. The shape and deformation of an echinocyte

Echinocytic shapes are characterised by a certain number of spicules, which because of their evaginated forms have large values of ΔA_0. In the formation of the echinocyte spicules, the relatively flat parts of the relaxed skeleton have to be displaced into more highly curved spicule regions. For the transformation of cell shape from discocyte to echinocyte, several studies have recognised that both skeleton shear elasticity and bilayer-bending elasticity must be considered to account for stable spicule formation properly. Early studies of this problem treated membrane skeleton as incompressible [18,23], but a more recent report extended the treatment to include the elastic compression and dilation of the skeleton [5]. Lim et al. [6] have recently shown that the whole stomatocyte–discocyte–echinocyte shape series is well accounted for by the equilibrium area difference changes and, in this way, they provided a theoretical support to the bilayer couple hypothesis of RBC shape transformations [8]. Some of their RBC shapes obtained theoretically are presented in Fig. 1D.

We have performed [7] corresponding studies of the echinocyte deformability. Previous studies of the effect of morphology on RBC deformability have already shown that echinocytic as well as stomatocytic shape alterations lead to decreased RBC deformability relative to the deformability of a discocyte [24–27]. We investigated the role of the equi1ibrium area difference ΔA_0 in the mechanical stiffness of the RBC. Experimentally, we modified RBC equilibrium area difference ΔA_0 by the method described by Artmann et al. [28], to produce RBC morphology changes of different degrees. Then, we examined RBC deformability by whole cell micropipette aspiration. An example of such an experiment is shown in Fig. 3. These results were compared with the results of the analysis of the cell deformation as it is aspirated into the pipette, where we used a parametric model to describe the shape of the partially aspirated cell and accounted for both the membrane skeletal and bilayer contributions to the energy.

RBC deformability measured by micropipette aspiration is characterised by the dependence of the equilibrium projection length on the aspiration pressure. For a certain cellular volume, cellular surface area and given material properties, the dependence of projection length on pressure can be

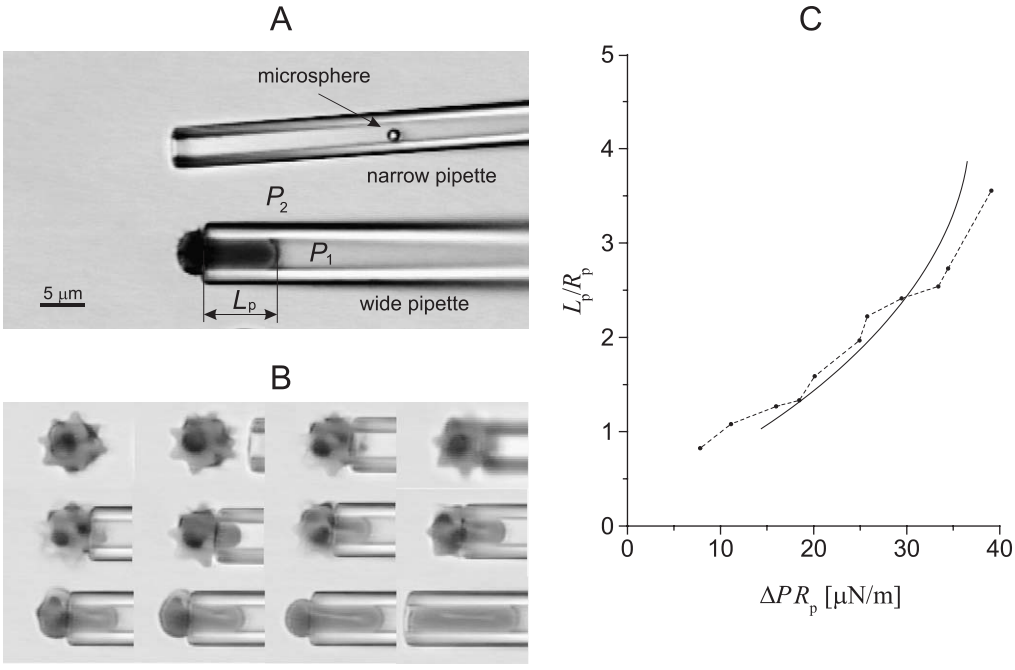

Fig. 3. The aspiration of the echinocyte into a large micropipette. The details of the experiment and analysis are described in Kuzman et al. [7]. (A) Two pipettes are used. Large aspiration pressures (ΔP>10 mm H_2O) were used to cause cell crenation via the smaller pipette ($R_p \sim 0.7$ μm). Small pressures (ΔP<3.0 mm H_2O) were applied via the larger pipette ($R_p \sim 1.7$ μm) to measure cell deformability. (B) Aspirated echinocytes at increasing aspiration pressures from the left to the right. (C) Experimentally obtained (points) and predicted (full line) dependence of the projection length (normalized by the pipette radius) on the product of the aspiration pressure times the pipette radius. The material constants are: $\mu = 6$ μN/m, $K = 2\mu$, $k_c = 2 \times 10^{-19}$ J, $k_r = 4k_c$, $V_0 = 109$ μm^3 and $A_0 = 140$ μm^2. The pipette radius is 1.7 μm.

obtained [7] and an example of the resultant fit is presented in Fig. 3B. It can be noted that the measured projection lengths (points in the figure) increase progressively with increasing aspiration pressure and at a certain aspiration pressure reach a critical value where the projection length begins to increase freely at constant pressure, i.e., the cell flows into the pipette without further increases in pressure. The model prediction (solid line) supports this behaviour. The model also predicted [7] that the surface density of the spicules in the outside portion of the cell decreases with increasing aspiration pressure, as can be noted in Fig. 3A by comparing the consecutive aspiration stages.

The progressively increasing deformability curve in Fig. 3B reflects two competitive skeleton deformation effects that occur during the aspiration of an echinocyte into a pipette: one due to the deformation in the spicules and the other due to the deformation in the pipette. The skeleton is initially "caught" in the higher deformation regions of the spicules. At small aspiration pressures, it is less favourable for the skeleton to be moved from spicules into the aspirated part of the membrane, causing the skeleton to be relatively compressed in the region outside the pipette and expanded in the aspirated portion. This results in an extra resistance to aspiration of the cell into the pipette. However, when the deformation in the aspirated portion is larger (near the critical point), the balance shifts toward higher density in the aspirated portion, leading to easier aspiration of the cell as the skeleton shifts from the spicules to the aspirated portion.

Comparison of the aspiration curves for the echinocytes of different echinocytic stages demonstrates [7] that the relationship between projection length and aspiration pressure depends on ΔA_0. The effect of an increase of ΔA_0 is a shift of the curve to larger values of the aspiration pressure (ΔPR_p) and a decrease in the slope of the curve. The critical point also depends on ΔA_0. Increasing ΔA_0 moves the critical point to larger values of ΔPR_p and smaller values of L_p/R_p.

5. Conclusions and implications

The RBC membrane is a composite of lipid bilayer and an underlying protein skeleton, and the mechanical properties of this composite are the principal determinants of cell morphology and the response of the cell to external forces. The elastic behaviour of the cell membrane includes contributions from the local and nonlocal bending of the bilayer as well as the shear and area expansivity of the membrane skeleton, subject to the constraint of constant membrane surface area. In the absence of time-dependent effects, these contributions to the membrane elastic energy constitute a minimal but complete model for the analysis of RBC shapes and deformability [5–7]. The role of the skeleton is particularly important in shape transformations and deformations that require large shear deformations, such as occur in the formation of an echinocyte or in the pipette aspiration experiment. In both cases, the skeletal and bilayer elasticity have to be included. We specifically demonstrated [7] that the relationship between cell deformability and the degree of crenation can be attributed solely to the modification of the bilayer equilibrium area difference ΔA_0.

Several inferences can be made with regard to the role of the membrane skeleton in the RBC mechanical stability. In the circulation, RBCs are subject to different stresses, which may jeopardise their integrity. A particular threat for the integrity of RBC is to attain a shape that is a composite of different spherical parts connected by narrow necks. Such shapes are found with simple phospholipid vesicles (the rightmost shapes in Fig. 1B and C, respectively) and also in RBCs heated to temperatures close to the thermal transition for spectrin [29]. It seems that the functional role of the RBC membrane skeleton is to prevent the formation of shapes containing buds. Previously, we already ascribed the role of the skeleton to this purpose by noting [30] that the skeleton prevents the formation of buds by inhibiting the segregation of membrane integral proteins, as would occur if the latter were free to diffuse laterally [31]. The present analysis points to another mechanism, resulting from the fact that skeleton shear deformation resulting from large changes of the circumferential dimensions of a budding region of the membrane is energetically unfavorable. Thus, the integrity of the RBC is preserved under conditions in which external perturbations might cause a temporary increase in the difference between the equilibrium areas of bilayer leaflets. The echinocyte RBC shape can thus be understood as a practical response of the cell that preserves its ability to function.

References

[1] A. McGough, Membrane skeleton: how to build a molecular shock absorber, Curr. Biol. 9 (1999) R887–R889.
[2] D.E. Discher, New insights into erythrocyte membrane organization and microelasticity, Curr. Opin. Hematol. 7 (2000) 117–122.
[3] N. Mohandas, E.A. Evans, Mechanical properties of the red cell membrane in relation to molecular structure and genetic defects, Annu. Rev. Biophys. Biomol. Struct. 23 (1994) 787–818.
[4] S.K. Boey, D.H. Boal, D.E. Discher, Simulations of the erythrocyte cytoskeleton at large deformation, I. Microscopic models, Biophys. J. 75 (1998) 1573–1583.
[5] R. Mukhopadhyay, G. Lim, M. Wortis, Echinocyte shapes: bending, stretching, and shear determine bump shape and spacing, Biophys. J. 82 (2002) 1756–1772.
[6] G.H.W. Lim, M. Wortis, R. Mukhopadhyay, Stomatocyte–discocyte–echinocyte sequence of the human red blood cell: evidence for the bilayer-couple hypothesis from membrane mechanics, Proc. Natl. Acad. Sci. U. S. A. 99 (2002) 16766–16769.
[7] D. Kuzman, S. Svetina, R.E. Waugh, B. Žekš, Determination of the echinocytic red blood cell deformability, Eur. Biophys. J., 2003. (doi:10.1007/S00249-003-0337-4)
[8] M.P. Sheetz, S.J. Singer, Biological membranes as bilayer couples—molecular mechanism of drug erythrocyte interactions, Proc. Natl. Acad. Sci. U. S. A. 71 (1974) 4457–4461.
[9] M. Bessis, Red cell shapes. An illustrated classification and its rationale, in: M. Bessis, R.I. Weed, P.F. Leblond (Eds.), Red Cell

Shape—Physiology, Pathology, Ultrastructure, Springer, Berlin Heidelberg New York, 1973, pp. 1–24.
[10] J. Käs, E. Sackmann, Shape transitions and shape stability of giant phospholipid vesicles in pure water induced by area-to-volume changes, Biophys. J. 60 (1991) 828–844.
[11] V. Heinrich, S. Svetina, B. Žekš, Nonaxisymmetric vesicle shapes in a generalized bilayer-couple model and the transition between oblate and prolate axisymmetric shapes, Phys. Rev., E 48 (1993) 3112–3123.
[12] L. Miao, U. Seifert, M. Wortis, H.G. Döbereiner, Budding transitions of fluid-bilayer vesicles: the effect of the area difference elasticity, Phys. Rev., E 49 (1994) 5389–5407.
[13] W. Helfrich, Blocked lipid exchanges in bilayers and its possible influence on the shape of vesicles, Z. Naturforsch. 29c (1974) 510–515.
[14] E.A. Evans, Minimum energy analysis of membrane deformation applied to pipet aspiration and surface-adhesion of red-blood-cells, Biophys. J. 30 (2) (1980) 265–284.
[15] S. Svetina, M. Brumen, B. Žekš, Lipid bilayer elasticity and the bilayer couple interpretation of the red cell shape transformations and lysis, Stud. Biophys. 110 (1985) 177–184.
[16] B. Božič, S. Svetina, B. Žekš, R.E. Waugh, Role of membrane structure in tether formation from bilayer vesicles, Biophys. J. 61 (1992) 963–973.
[17] K.A. Brakke, The surface evolver, Exp. Math. 1 (1992) 141–165.
[18] R.E. Waugh, Elastic energy of curvature-driven bump formation on red blood cell membrane, Biophys. J. 70 (1996) 1027–1035.
[19] E.A. Evans, New membrane concept applied to the analysis of fluid shear- and micropipette-deformed red blood cells, Biophys. J. 13 (1973) 941–954.
[20] D.E. Discher, N. Mohandas, E.A. Evans, Molecular maps of red-cell deformation: hidden elasticity and in situ connectivity, Science 266 (1994) 1032–1035.
[21] C.D. Eggleton, A.S. Popel, Large deformation of red blood cell ghosts in a simple shear flow, Phys. Fluids 10 (1998) 1834–1845.
[22] D.E. Discher, D.H. Boal, S.K. Boey, Simulations of the erythrocyte cytoskeleton at large deformation: II. Micropipette aspiration, Biophys. J. 75 (1998) 1584–1597.
[23] A. Iglič, A possible mechanism determining the stability of spiculated red blood cells, J. Biomech. 30 (1997) 35–40.
[24] H.J. Meiselman, Morphological determinants of red cell deformability, Scand. J. Clin. Lab. Invest. 41 (Suppl. 156) (1981) 27–34.
[25] W.H. Reinhart, S. Chien, Red cell rheology in stomatocyte–echinocyte transformation: roles of cell geometry and cell shape, Blood 67 (1986) 1110–1118.
[26] A. Chabanel, W. Reinhart, S. Chien, Increased resistance to membrane deformation of shape-transformed human red blood cells, Blood 69 (1987) 739–743.
[27] G. Bazzoni, M. Rasia, Effects of an amphipathic drug on the rheological properties of the cell membrane, Blood Cell Mol. Diseases 24 (1998) 552–559.
[28] G.M. Artmann, K.L.P. Sung, T. Horn, D. Whittemore, G. Norwich, C. Shu, Micropipette aspiration of human erythrocytes induces echinocytes via membrane phospholipid translocation, Biophys. J. 72 (1997) 1434–1441.
[29] W.T. Coakley, A.J. Bater, J.O.T. Deeley, Vesicle production on heated and stressed erythrocytes, Biochim. Biophys. Acta 512 (1978) 318–330.
[30] S. Svetina, A. Iglič, V. Kralj-Iglič, B. Žekš, Cytoskeleton and red cell shape, Cell. Mol. Biol. Lett. 1 (1996) 67–78.
[31] J. Simon, M. Kühner, H. Ringsdorf, E. Sackmann, Polymer-induced shape changes and capping in giant liposomes, Chem. Phys. Lipids 76 (1995) 241–258.